

# Accurate Small Models using Adaptive Sampling

Abhishek Ghose\*

## Abstract

We highlight the utility of a certain property of model training: instead of drawing training data from the same distribution as test data, learning a different training distribution often improves accuracy, especially at small model sizes. This provides a way to build accurate small models, which are attractive for interpretability and resource-constrained environments. Here we empirically show that this principle is both general and effective: it may be used across tasks/model families, and it can augment prediction accuracy of traditional models to the extent they are competitive with specialized techniques. The tasks we consider are explainable clustering and prototype-based classification. We also look at Random Forests to illustrate how this principle may be applied to accommodate multiple size constraints, e.g., number of trees and maximum depth per tree. Results using multiple datasets are presented and are shown to be statistically significant.

## 1 Introduction

We demonstrate the utility of a certain property of model training: instead of drawing training data from the same distribution as test data, learning a different training distribution often improves accuracy, typically at small model sizes. This has been earlier shown to be true across multiple model families [13, 14]. Additionally, it was shown that as model sizes increase, the ideal training distribution approximates the test distribution (the commonly known case). This phenomenon is leveraged to construct accurate small models: low accuracy due to constrained model size is compensated by learning a training distribution.

Figure 1 illustrates this phenomenon. The  $x$ -axis shows model size ( $depth$  of decision trees, normalized to  $(0, 1]$ ) and the  $y$ -axis shows the fraction of ideal training data that comes from the same distribution as the test data<sup>1</sup>. We note that: (a) for low values of  $x$ ,  $y$  takes on a range of values, and (b)  $x \rightarrow 1 \Rightarrow y \approx 1$ .

\*Department of Computer Science and Engineering, IIT Madras, Chennai, India

<sup>1</sup>Values for this fraction come from a parameter in their framework that allows the model to mix data from these sources: (a) uniformly sampled from the original training dataset (b) a learned distribution.

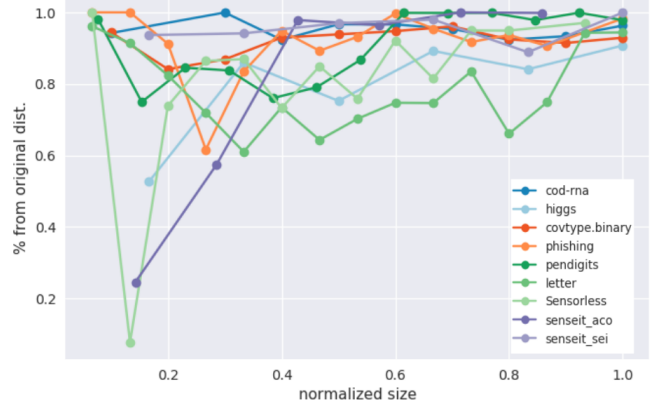


Figure 1: Reproduced from [14]. As model size increases ( $x$ -axis), the ideal training sample progressively favors the same distribution as the test data. Different lines represent different datasets. The model used here is a decision tree, where its  $depth$  acts as size.

The techniques presented in [13, 14] maybe seen as forms of “adaptive sampling”, since they learn training distribution parameters by iteratively adapting them to maximize held-out accuracy. For the purpose of discussion, we refer to them as “**Compaction by Adaptive Sampling**” (COAS).

Our contribution is to highlight the utility of this phenomenon:

1. While earlier work studies its effect for a given model family, here we ask if such improvements are competitive for a *task*, i.e., when compared with specialized techniques.

For example, we show that cluster explanation trees produced by applying COAS to the CART algorithm [5] (proposed in 1993), improves its performance to the degree that it is competitive with *Iterative Mistake Minimization (IMM)* [21] (proposed in 2020), which is *specifically designed* for this task.

Similar comparisons are presented for prototype-based classification.

2. Positive results are also presented for the case when model size is not scalar: we consider the case of Random Forests (RF) where *both* number of trees in the forest and maximum depth of each tree are constrained. The case of vector size is briefly discussed in [13] (for the case of Gradient Boosted Machines); here we rigorously analyze the case for RFs.

In presenting these results, our goal is to draw attention to both the *generality* and *effectiveness* of the principle of *learning* a training distribution to improve accuracy. Accurate small models are attractive for interpretability and for use in resource-constrained environments today; and therefore, we believe that awareness of such a powerful model-agnostic strategy, that is currently under-utilized, may be of immense practical value.

The remainder of the paper is structured as follows: In Section 2, we provide an overview of COAS, since its understanding is central to this work. In sections, Section 3 and 4, we measure the competitiveness of COAS at the tasks of *Explainable Clustering* and *prototype-based classification* respectively. This is done by augmenting a “traditional” technique using COAS, and showing it to be competitive to task-specific techniques. In Section 5, we show that COAS is also effective when the notion of model size is a vector, such as in the case of RFs, where number of trees and maximum depth per tree jointly identify model size. A discussion of our findings and of directions of future work in Section 6 concludes the paper.

## 2 Overview

We present an overview of COAS in this section; specifically, we discuss the algorithm in [13], and not the one presented in [14], since the former was shown to be more accurate. We simplify some aspects for brevity - for details please see [13].

COAS learns a sampling distribution over training data  $(X_{tr}, y_{tr})$ , where  $X_{tr} \in \mathbb{R}^{N \times d}$ . Here,  $N$  is the size of the training set and  $d$  is dimensionality of data. The objective is to maximize classification accuracy, calculated by a user-specified scoring function, of a predictive model  $M$  on test data  $(X_{test}, y_{test})$ . The training algorithm  $f$  that produces  $M$  and model size  $\eta$  (a constraint that applies to  $M$ ) are also inputs to COAS. The sample size  $N_s$  that  $f$  uses is learned by COAS, provided user-specified lower and upper bounds. Examples of  $M$ ,  $f$  and  $\eta$  are decision tree, the CART training algorithm and depth of a decision tree, respectively.

Directly modeling  $p(x_i), x_i \in X_{tr}$  is avoided since

such a distribution may become computationally expensive at high dimensions. Instead, COAS learns a distribution over *prediction uncertainties*  $u_i \in [0, 1], 1 \leq i \leq N$ , as computed by a powerful “oracle” model. The uncertainty values  $u_i$ , collectively denoted as  $U_{tr} \in \mathbb{R}^{N \times 1}$ , may be seen as an *one-dimensional projection* of  $X_{tr}$ , that is sufficiently informative for this problem. The oracle may be any powerful probabilistic classifier, and results for *Gradient Boosted Machines*, *Random Forest* and *Gated Recurrent Unit* are provided in [13].

We denote the distribution over uncertainties as  $P(u_i; \theta)$ . This is iteratively learned (along with the optimal sample size  $N_s$ ) over  $T$  iterations by an optimizer.

Algorithm 1 depicts the technique. The optimizer is referred to as *suggest*. Box constraints for  $\theta$  and  $N_s$ , denoted by  $B_\theta$  and  $B_{N_s}$  respectively, are also required as inputs.

---

### Algorithm 1 Abstracted view of COAS.

---

**Require:**  $(X_{tr}, U_{tr}, y_{tr})$ ,  $(X_{val}, y_{val})$ ,  $(X_{test}, y_{test})$ , training algorithm  $f$ , model size  $\eta$ , scoring function *score*, optimization budget  $T$ , box constraints  $B_\theta, B_{N_s}$  for  $\theta, N_s$  respectively.

- 1: Initialize:  $acc^* \leftarrow 0, M^* \leftarrow 0, N_{s_0} \in B_{N_s}, \theta_0 \in B_\theta, \mathcal{H} \leftarrow \{(\theta_0, N_{s_0}, \cdot)\}$
- 2: **for**  $t \leftarrow 1$  **to**  $T$  **do**
- 3:    $(\theta_t, N_{s_t}) \leftarrow suggest(\mathcal{H})$
- 4:    $S \leftarrow \{(x_{jk}, y_{jk})\}$  where  $p((x_{jk}, y_{jk})) = p(u_{jk}; \theta_t)$ ,  $|S| = N_{s_t}$  and  $(x_{jk}, y_{jk}) \in (X_{tr}, y_{tr})$
- 5:    $M_t \leftarrow f(S, \eta)$
- 6:    $acc_t \leftarrow score(M_t(X_{val}), y_{val})$
- 7:   **if**  $acc_t > acc^*$  **then**
- 8:      $M^* \leftarrow M_t$
- 9:   **end if**
- 10:    $\mathcal{H} \leftarrow \mathcal{H} \cup \{(\theta_t, N_{s_t}, acc_t)\}$
- 11: **end for**
- 12:  $acc_{test} \leftarrow score(M^*(X_{test}), y_{test})$
- 13: **return**  $M^*, acc_{test}$

---

Some relevant properties of Algorithm 1 are:

1. The validation and test data remain unchanged through the algorithm.
2. It is model agnostic, i.e.,  $f$  is assumed to be a black-box function.
3. It is shown to produce good results with default settings  $B_\theta$  and  $B_{N_s}$ , and the only hyperparameter that needs to be set in practice is the optimization budget  $T$ .
4. The distribution parameter  $\theta$  is a vector that represents a combination of two distributions: (a)

uniform random sample from the  $(X_{tr}, y_{tr})$  (b) an *infinite mixture model* using a *Dirichlet Process*, defined over  $u_i$ . Their relative proportion in sample  $S$  is also determined by  $\theta$ .

5. Since the optimizer needs to work with a black-box function  $f$ , *suggest* is implemented using *Bayesian Optimization (BO)*.

Given a history  $\mathcal{H}$  of values for  $\theta$ ,  $N_s$  and *acc* from prior iterations, it offers the best next guess for  $\theta$  and  $N_s$ . Their initial values for  $\theta$  and  $N_s$  may be randomly picked<sup>2</sup> from their search spaces,  $B_\theta$  and  $B_{N_s}$ , and the initial value for *acc* is computed based on this selection (shown as a “.” in line 1, to denote its determined by  $\theta_0, N_{s_0}$ , similar to line 6).

6. For instance  $x_i$ , uncertainty  $u_i$  is calculated as  $1 - (p(c_u|x_i) - p(c_v|x_i))$ , where  $p(c|x_i)$  is the probability of  $x_i$  belonging to class  $c$  as per the oracle, and  $c_u$  and  $c_v$  are classes with the highest and next highest probabilities, respectively. The quantity  $p(c_u|x_i) - p(c_v|x_i)$  is known as the *margin* [25].

For our experiments, we use the reference Python implementation: *compactem* [12]. GBM models, constructed using the *LightGBM* [17] library, are used as oracles. These are calibrated using *Platt scaling* [24]. We use the default BO optimizer made available in the implementation: *Tree Structured Parzen Estimator (TPE)* [3, 16].

### 3 Explainable Clustering

The first task we investigate is the problem of *Explainable Clustering*. Introduced by [21], the goal is to explain cluster allocations as discovered by techniques such *k-means* or *k-medians*. This is achieved by constructing axis-aligned decision trees with leaves that either exactly correspond to clusters, e.g., *Iterative Mistake Minimization (IMM)* [21], or are proper subsets, e.g., *Expanding Explainable k-Means Clustering (ExKMC)* [11]. We consider the former case here, i.e., a tree must possess exactly  $k$  leaves to explain  $k$  clusters.

We denote a specific clustering by  $C$ . If the assigned cluster for an instance  $x_i, i = 1 \dots N$ , is denoted by  $C(x_i)$  where  $C(x_i) \in \{1, 2, \dots, k\}$ , and the cluster centroids are denoted by  $\mu_j, j = 1, \dots, k$ , then the cost of clustering  $C$  is given by:

$$(3.1) \quad C = \frac{1}{N} \sum_{j=1}^k \sum_{\{x_i | C(x_i) = \mu_j\}} \|x_i - \mu_j\|_2^2$$

<sup>2</sup>In practice, random initialization is not performed - see [13] - but that detail is not relevant here.

In the case of an explanation trees with  $k$  leaves,  $\mu_j$  are centroids of leaves. Cluster explanation techniques attempt to minimize this cost.

The price of interpretability maybe measured as the *cost ratio*:

$$(3.2) \quad \text{cost ratio} = \frac{C_{Ex}}{C_{KM}}$$

Here  $C_{Ex}$  is the cost achieved by an explanation tree, and  $C_{KM}$  is the cost obtained by a standard k-means algorithm. We refer to this ratio as the *cost ratio*; it assumes values in the range  $[1, \infty]$ , where the lowest cost is obtained when using k-means, i.e.,  $C_{Ex}$  and  $C_{KM}$  are the same.

One may also indirectly minimize the cost in the following manner: use k-means to produce a clustering, use the cluster allocations of instances as their labels, and then learn a standard decision tree for classification, e.g., CART. This approach has been shown to be often outperformed by tree construction algorithms that directly minimize the cost in Equation 3.1.

**Algorithms and Hyperparameters:** The algorithms we compare and their hyperparameter settings are as follows:

1. **Iterative Mistake Minimization (IMM)** [21]: This generates a decision tree via greedy partitioning using a criterion that minimizes number of mistakes at each split (the number of points separated from their corresponding reference cluster center). There are no parameters to tune. We used the implementation available here: <https://github.com/navefr/ExKMC>, which internally uses the reference implementation for IMM.
2. **ExShallow** [20]: Here, the decision tree construction explicitly accounts for minimizing explanation complexity while targeting a low cost ratio. The trade-off between clustering cost and explanation size is controlled via a parameter  $\lambda$ . This is set as  $\lambda = 0.03$  in our experiments; this value is used in the original paper for various experiments. We used the reference implementation available here: <https://github.com/lmurtinho/ShallowTree>.
3. **COAS**: We use CART [5] as the traditional model to compare, and maximize the classification accuracy for predicting clusters, as measured by the F1-macro score. The implementation in *scikit* [23] is used. During training, we set the following parameters: (a) the maximum number of leaves (this represents *model size*  $\eta$  here) is set to the number of clusters  $k$ , and (b) the parameter *class.weight* is set to “*balanced*” for robustness to disparate cluster sizes. Results for CART are denoted with label

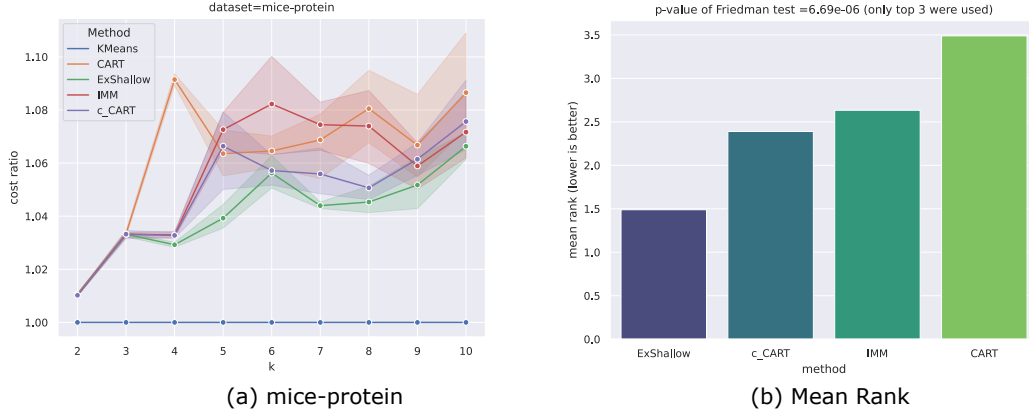


Figure 2: Comparisons over explainable clustering algorithms are shown. (a) shows the comparison for a specific dataset *mice-protein*. (b) shows mean ranks of these techniques over five datasets; the Friedman test is conducted over the **top three** techniques only, with  $p = 6.688 \times 10^{-6}$ . See Supplementary document for additional plots.

**CART.** We then apply COAS to CART; these results are denoted as **c\_CART** (“c-” for *compact*). We set  $T = 2000$ , and use default settings for other parameters, e.g.,  $N_s \in [400, |X_{train}|]$ . Since we are explaining clusters (and not predicting on unseen data), the training, validation and test sets are identical.

**Experiment setup:** The comparison is performed over five datasets (limited to 1000 instances), and for each dataset,  $k = 2, 3, \dots, 10$  clusters are produced. Results for the cost ratio (Equation 3.2) are reported over *five* trials. Evaluations are performed over the following publicly available datasets: *avila*, *covtype*, *covtype.binary*, *Sensorless* [7] and *mice-protein* [9]. We *specifically picked* these datasets since CART is known to perform poorly on them [11, 20].

**Observations:** Figure 2 presents our results. Figure (a) shows the plot for the *mice-protein* dataset: the 95% confidence interval, in addition to cost ratio, is shown. Plots for other datasets maybe found in the Supplementary document. The cost for k-means is shown for reference. Figure 2 (b) shows the *mean ranks* of the various techniques (lower is better) across datasets and number of clusters (trials are aggregated over), and its title shows the  $p$ -value =  $6.688 \times 10^{-6}$  of a *Friedman test* conducted over the *top three techniques*: we restrict the test to top candidates since otherwise it would be very easy to obtain a low/favorable score, due to the high numbers for CART. The low score indicates with high confidence that ExShallow, IMM and c\_CART do not produce the same outcomes.

From the plot of mean ranks in Figure 2(b), we observe that although CART performs quite poorly, the

application of COAS drastically improves its performance, to the extent that it competes favorably with techniques like IMM and ExShallow; its mean rank places it between them. This is especially surprising given that it doesn’t explicitly minimize the cost in Equation 3.1. We also note the following  $p$ -values from *Wilcoxon signed-rank* [26] tests:

- CART vs c\_CART:  $p = 1.4783 \times 10^{-6}$ . The low value indicates that using COAS indeed significantly changes the accuracy of CART.
- IMM vs c\_CART:  $p = 0.0155$ . The relatively high value indicates that the performance of c\_CART is competitive with IMM.

Here, both the Friedman and Wilcoxon tests are performed for combinations of datasets and  $k$ , e.g., *avila-2*, *avila-3*, *covtype-10*, and scores across trials for a combination are averaged.

#### 4 Prototype-based Classification

Next, we consider prototype-based classification. At training time, such techniques identify “prototypes” within the data (actual training instances or generated instances), that maybe used to classify a test instance based on their similarity to them. A popular technique in this family is the *k-Nearest Neighbor* (*kNN*). These are simple to interpret, and if a small but effective set of prototypes maybe identified, they can be convenient to deploy on edge devices [15, 27]. Research in this area has focused on minimizing the number of prototypes that need to be retained while minimally trading off accuracy.

We define some notation first. The number of prototypes, which is an input to our experiments, is denoted by  $N_p$ . We will also use  $K_\gamma(x_i, x_j) = e^{-\gamma \|x_i - x_j\|_2^2}$  to denote the *Radial Basis Function (RBF) kernel*, parameterized by the kernel bandwidth  $\gamma$ .

**Algorithms and Hyperparameters:** These are the algorithms we compare:

1. **ProtoNN** [15]: This technique uses a RBF kernel to aggregate influence of prototypes. Synthetic prototypes are learned and additionally a “score” is learned for each of them that designates their contribution towards *each* class. The prediction function sums the influence of neighbors using the RBF kernel, weighing contribution towards each class using the learned score values; the class with the highest total score is predicted. The method also allows for reducing dimensionality, but we don’t use this aspect<sup>3</sup>. The various parameters are learned via gradient based optimization.

We use the *EdgeML* library [8], which contains the reference implementation for ProtoNN. For optimization, the implementation uses the version of *ADAM* [18] implemented in *TensorFlow* [1]; we set *num\_epochs* = 200, *learning\_rate* = 0.05, while using the defaults for other parameters. The *num\_epochs* and *learning\_rate* values are picked based on a limited search among values {100, 200, 300} and {0.01, 0.05} respectively. The search space explored for  $\gamma$  is [0.001, 0.01, 0.1, 1, 10]. Defaults are used for the other ProtoNN hyperparameters.

2. **Stochastic Neighbor Compression (SNC)** [19]: This also uses a RBF kernel to aggregate influence of prototypes, but unlike ProtoNN, the prediction is performed via the *1NN rule*, i.e., prediction uses only the nearest prototype. The technique bootstraps with randomly sampled  $N_p$  prototypes (and corresponding labels) from the training data, and then modifies their coordinates for greater accuracy using gradient based optimization; the labels of the prototypes stay unchanged in this process. This is another difference compared to ProtoNN, where in the latter each prototype contributes to all labels to varying extents. The technique maybe extended to reduce the dimensionality of the data (and prototypes); we don’t use this aspect.

<sup>3</sup>The implementation provides no way to switch off learning a projection, so we set the dimensionality of the projection to be equal to the original number of dimensions. This setting might however learn a transformation of the data to space within the same number of dimensions, e.g., translation, rotation.

We were unable to locate the reference implementation mentioned in the paper, so we implemented our own version, with the help of the *JAXopt* library [4]. For optimization, gradient descent with *backtracking line search* is used. A total of 100 iterations for the gradient search is used (based on a limited search among these values: {100, 200, 300}), and each backtracking search is allowed up to 50 iterations. A grid search over the following values of  $\gamma$  is performed: [0.001, 0.01, 0.1, 1, 10].

3. **Fast Condensed Nearest Neighbor Rule** [2]: Learns a “consistent subset” for the training data: a subset such that for any point in the training set (say with label  $l$ ), the closest point in this subset also has a label  $l$ . Of the multiple variations of this technique proposed in [2], we use **FCNN1**, which uses the 1NN rule for prediction. There are no parameters to tune. We used our own implementation.

A challenge in benchmarking this technique is it *does not* accept  $N_p$  as a parameter; instead it iteratively produces expanding subsets of prototypes until a stopping criteria is met, e.g., if prototype subsets  $V_i$  and  $V_{i+1}$  are produced at iterations  $i$  and  $i+1$  respectively, then  $V_i \subset V_{i+1}$ . For comparison, we consider the performance at iteration  $i$  to be the result of  $N_p$  prototypes where  $N_p \leftarrow |V_i|$ .

4. **COAS**: For the traditional model, we use *Radial Basis Function Networks (RBFN)* [6]. For a binary classification problem with classes  $\{-1, 1\}$ , given prototypes  $x_i, i = 1, 2, \dots, p$ , the label of a test instance  $x$  is predicted as  $\text{sgn}(\sum_i w_i K_\gamma(x, x_i))$  (label 1 is predicted for a score of 0). Weights  $w_i$  are learned using linear regression. A one-vs-rest setup is used for multiclass problems. For our baseline, we use cluster centres of a *k-means* clustering with  $k \leftarrow N_p$ , as our prototypes. These results are denoted using the term **KM-RBFN**. In the COAS version, denoted by **c-RBFN**, the  $N_p$  prototypes are sampled from the training data.  $N_p$  represents *model size*  $\eta$  here.

Note that the standard RBFN, and therefore the variants used here KM-RBFN and c-RBFN, don’t provide a way to reduce dimensionality; this is the reason why this aspect of ProtoNN and SNC wasn’t used (for fair comparison).

For COAS, we set  $T = 1000$  and  $N_s$  was set to  $[N_p - 1, N_p]$  to get the desired number of prototypes<sup>4</sup>

<sup>4</sup>The implementation [12] doesn’t allow for identical lower and upper bounds, hence the lower bound here is  $N_p - 1$ .

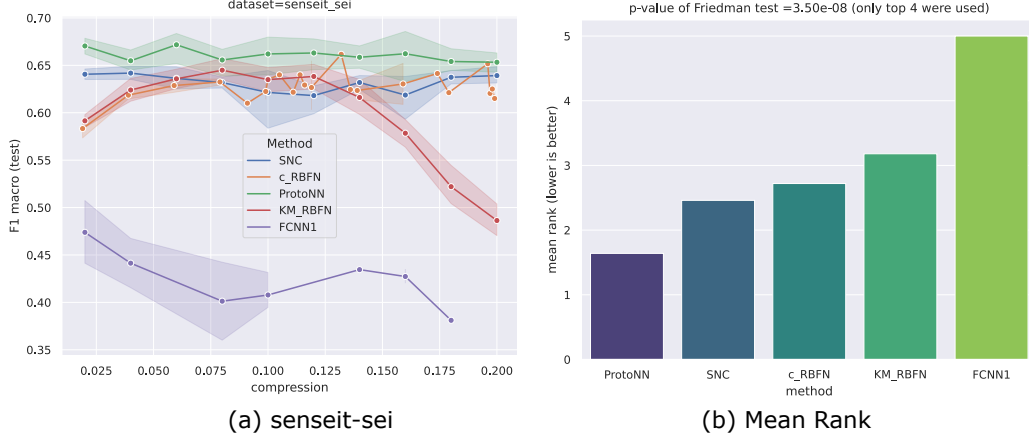


Figure 3: Various prototype-based classifiers are compared. (a) shows comparison for the dataset *senseit-sei*. Number of prototypes are shown as percentage of the training data on the *x-axis*. (b) shows the mean ranks of techniques based on five datasets; the Friedman test is conducted over the **top four** techniques only, with  $p = 3.5025 \times 10^{-8}$ . See Supplementary document for additional plots.

Although all the above techniques use prototypes for classification, it is interesting to note variations in their design: ProtoNN, SNC, KM\_RBFN use synthetic prototypes, i.e., they are not part of the training data, while c\_RBFN and FCNN1 select  $N_p$  instances from the training data. The prediction logic also differs: ProtoNN, KM\_RBFN, c\_RBFN derive a label from some function of the influence by all prototypes, while SNC and FCNN1 use the 1NN rule.

**Experiment setup:** As before, we evaluate these techniques over five standard datasets: *adult*, *covtype.binary*, *senseit-sei*, *senseit-aco*, *phishing* [7]. 1000 training points are used, with  $N_p \in \{20, 40, 60, 80, 100, 140, 160, 180, 200\}$ . Results are reported over five trials. The score reported is the F1-macro score.

**Observations:** Results are shown in Figure 3. (a) shows the plot for the *senseit-sei* dataset. The number of prototypes are shown on the *x-axis* as *percentages* of the training data. Plots for other datasets may be found in the Supplementary document. Figure 3 (b) shows the mean rank (lower is better) across datasets and number of prototypes (trials are aggregated over). The p-value of the Friedman test is reported,  $p = 3.5025 \times 10^{-8}$ . Here too, we do not consider the worst performing candidate, FCNN1 - so as to not bias the Friedman test in our favor.

We observe in Figure 3 that while both ProtoNN and SNC outperform c\_RBFN, the performance of SNC and c\_RBFN are close. We also observe that FCNN1 performs poorly; this matches the observations in [19].

We also consider the following *p-values* from

*Wilcoxon signed-rank* tests:

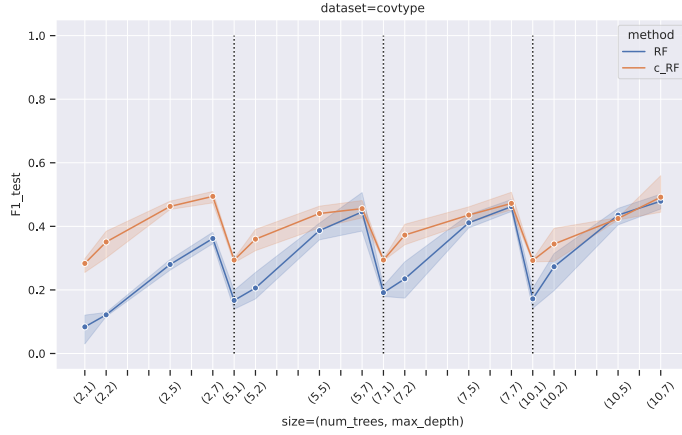
1. KM\_RBFN vs c\_RBFN:  $p = 1.699 \times 10^{-4}$ . The low value indicates COAS significantly improves upon the baseline KM\_RBFN.
2. SNC vs c\_RBFN:  $p = 0.1260$ . The relatively high value here indicates that c\_RBFN is competitive with SNC; in fact, at a confidence threshold of 0.1, their outcomes would not be interpreted as significantly different.

## 5 Random Forest

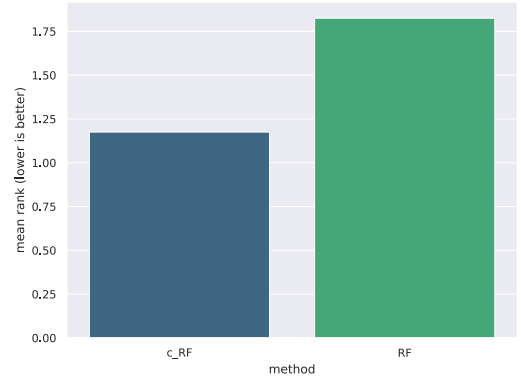
In the previous sections, we considered the case of scalar model sizes: number of leaves in the case of explanation trees for clustering (Section 3) and number of prototypes in the case of prototype-based classification (Section 4). Here, we assess the effectiveness of the technique when the model size is composed of multiple constraints. This is to demonstrate the generality of COAS across not just model families, but also the notion of model size.

We look at the case of learning *Random Forests* (RF) where we specify model size using *both* the number of trees and the maximum depth per tree.

**Algorithms and Hyperparameters:** We train RFs without and with COAS, denoted as **RF** and **c\_RF** respectively. For COAS, we set number of iterations as  $T = 3000$  and  $N_s \in [30, |X_{train}|]$  (the lower bound was obtained by limited search). The implementation in *scikit* is used, and for standard RF models, i.e., without COAS, the parameter *class\_weight* is set to “*balanced.subsample*” to make them robust to class imbalance.



(c) covtype



(f) Mean Rank

Figure 4: (a) shows results for the dataset=*covtype*. Plots for other datasets may be found in the Supplementary document. (b) provides mean ranks, but since there are only two models being compared, the Friedman test cannot be performed.

**Experiment setup:** We use the following five standard datasets for this experiment: *heart*, *Sensorless*, *covtype*, *ionosphere*, *breast cancer* [7]. For each dataset, all size combinations from the following sets are tested (three trials per combination):  $num\_trees \in \{2, 5, 7, 10\}$  and  $max\_depth \in \{1, 2, 5, 7\}$ . The total dataset size used was 3250 instances, with 70 : 30 split for train to test. We reported the F1-macro score.

**Observations:** Figure 4 (a) shows the results for dataset *covtype*; the  $x$ -axis shows values of the tuple  $(num\_trees, max\_depth)$  sorted by the first and then the second index. Plots for other datasets may be found in the Supplementary document. Figure 4 (b) shows mean ranks across datasets, number of trees and maximum tree depths (trials are aggregated over). A Friedman test cannot be performed since it requires at least three techniques to compare.

For a combination of dataset,  $num\_trees$  and  $max\_depth$ , a *Wilcoxon signed-rank* test yields  $p = 1.44 \times 10^{-11}$ , denoting a significant difference between results of RF and c\_RF .

## 6 Discussion

The above experiments demonstrate that the strategy of learning an optimal training distribution is both *general* and *effective*:

1. It may be applied to CART, RBFN or RFs.
2. It admits vector notion of sizes, e.g., for RFs in Section 5.
3. It can augment relatively old techniques to com-

pete with newer ones: in the case of explainable clustering, the augmented version of CART (proposed in 1993) is competitive with IMM (proposed in 2020), and in the case of prototype-based classification, augmented RBFNs (proposed in 1988) are competitive with SNC (proposed in 2014).

This substantiates our argument that this is a powerful model training principle for small-sized models.

While we are not aware of any theoretical work that analyzes this phenomena, and this work itself is empirical, we illustrate its operation in Figure 5, for the explainable clustering problem on a toy dataset with 500 instances. Figure 5(a) shows clusters discovered by *k-means* with  $k = 5$ . Points belonging to a cluster are shown by the same color, and cluster boundaries are shown using *convex hulls*. Figure 5(b) shows the leaf partitions learned by a standard CART tree, resulting in a cost ratio of 1.16. Finally Figure 5(c) shows the partitions learned by *c-CART* (with the settings  $T = 1000$  and  $N_s \in [30, 500]$ ). Here, both the size and opacity indicate the number of times a point was sampled in the final distribution: larger and relatively opaque points were sampled more. Crosses indicate instances that were ignored in the optimal sample; 59.80% of instances fall in this category. Thus, somewhat surprisingly, the optimal sample ignores more than half of the input. Note the shift in the leaf boundaries, especially the ones on the right and bottom of Figure 5(b) and (c). The new cost ratio is 1.09. A theoretical framework is a good direction for future work.



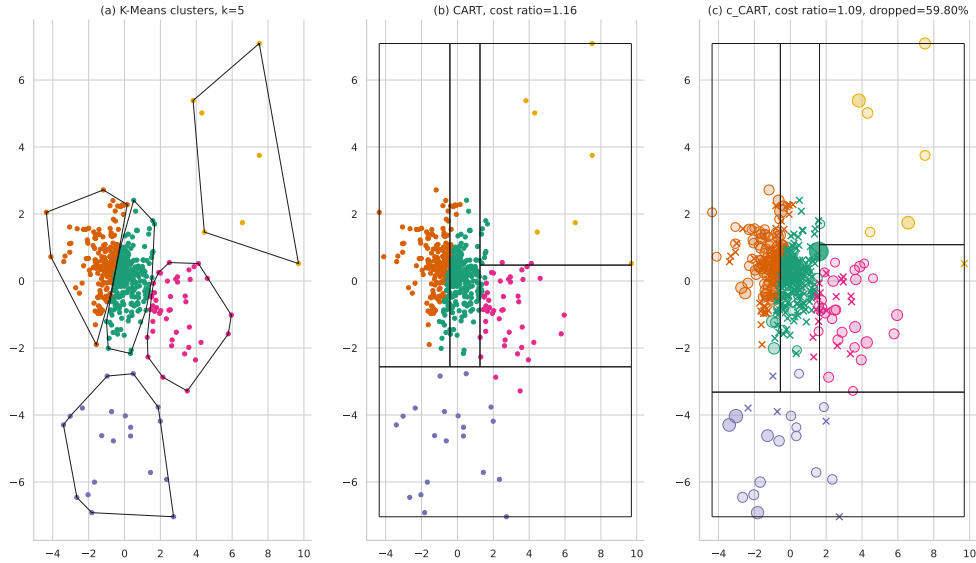


Figure 5: (a) shows the clusters discovered by k-means for  $k = 5$ . The cluster boundaries are visualized using convex hulls. (b) shows leaf partitions of a CART tree that mimics the clustering in (a); this has cost ratio 1.16. In (c), leaves of a c.CART tree are shown. Also, the sample weights of points are shown using size and the alpha value of face colours: larger and relatively opaque points have greater weights. The optimal sample also ignores some points - these are explicitly shown with  $\times$  markers. 59.80% of the points are ignored here. The cost ratio is 1.09. Note the change in the regions covered by the leaves on the right and bottom between (b) and (c).

We believe that it is equally important for us to call out what this paper is *not* claiming. We do not propose that COAS replace the techniques it was compared to without further analysis, as they may provide other task specific benefits, e.g., ExShallow targets certain specific explanation-quality metrics, aside from the cost ratio.

Instead, this work is a modest call to action to explore learning the training distribution as a general principle to improve small model accuracy. We believe this to be a relatively unknown phenomenon. Although the COAS algorithm is a good tool to utilize this strategy today, our primary message is the principle itself, independent of any specific algorithm. The principle might be implemented in other ways, possibly in a way that's better suited to a task of interest, and possibly in conjunction with other strategies. Some relevant directions for future work are: (a) learn weights for training instances (as opposed to a distribution) using *bilevel optimization* [22, 10] for the case of a differentiable training loss function (b) COAS itself may be improved with the use of a different black-box optimizer.

## References

- [1] M. ABADI, A. AGARWAL, P. BARHAM, E. BREVDO, Z. CHEN, C. CITRO, G. S. CORRADO, A. DAVIS, J. DEAN, M. DEVIN, S. GHEMAWAT, I. GOODFELLOW, A. HARP, G. IRVING, M. ISARD, Y. JIA, R. JOZEFOWICZ, L. KAISER, M. KUDLUR, J. LEVENBERG, D. MANÉ, R. MONGA, S. MOORE, D. MURRAY, C. OLAH, M. SCHUSTER, J. SHLENS, B. STEINER, I. SUTSKEVER, K. TALWAR, P. TUCKER, V. VANHOUCHE, V. VASUDEVAN, F. VIÉGAS, O. VINYALS, P. WARDEN, M. WATTENBERG, M. WICKE, Y. YU, AND X. ZHENG, *TensorFlow: Large-scale machine learning on heterogeneous systems*, 2015. Software available from tensorflow.org.
- [2] F. ANGIULLI, *Fast condensed nearest neighbor rule*, in Proceedings of the 22nd International Conference on Machine Learning, ICML '05, New York, NY, USA, 2005, Association for Computing Machinery, p. 25–32.
- [3] J. BERGSTRA, R. BARDENET, Y. BENGIO, AND B. KÉGL, *Algorithms for hyper-parameter optimization*, in Proceedings of the 24th International Conference on Neural Information Processing Systems, NIPS'11, USA, 2011, Curran Associates Inc., pp. 2546–2554.
- [4] M. BLONDEL, Q. BERTHET, M. CUTURI, R. FROSTIG, S. HOYER, F. LLINARES-LÓPEZ, F. PEDREGOSA, AND J.-P. VERT, *Efficient and modular implicit differentiation*, arXiv preprint arXiv:2105.15183, (2021).
- [5] L. BREIMAN ET AL., *Classification and Regression*



- Trees*, Chapman & Hall, New York, 1984.
- [6] D. BROOMHEAD AND D. LOWE, *Multivariable functional interpolation and adaptive networks*, Complex Systems, 2 (1988), pp. 321–355.
  - [7] C.-C. CHANG AND C.-J. LIN, *LIBSVM: A library for support vector machines*, ACM Transactions on Intelligent Systems and Technology, 2 (2011), pp. 27:1–27:27. Software available at <http://www.csie.ntu.edu.tw/~cjlin/libsvm>, datasets at <https://www.csie.ntu.edu.tw/~cjlin/libsvmtools/datasets/>.
  - [8] DENNIS, DON KURIAN AND GOPINATH, SRIDHAR AND GUPTA, CHIRAG AND KUMAR, ASHISH AND KUSUPATI, ADITYA AND PATIL, SHISHIR G AND SIMHADRI, HARSHA VARDHAN, *EdgeML: Machine Learning for resource-constrained edge devices*.
  - [9] D. DUA AND C. GRAFF, *UCI machine learning repository*, 2017.
  - [10] L. FRANCESCHI, P. FRASCONI, S. SALZO, R. GRAZZI, AND M. PONTIL, *Bilevel programming for hyperparameter optimization and meta-learning*, in Proceedings of the 35th International Conference on Machine Learning, J. Dy and A. Krause, eds., vol. 80 of Proceedings of Machine Learning Research, PMLR, 10–15 Jul 2018, pp. 1568–1577.
  - [11] N. FROST, M. MOSHKOVITZ, AND C. RASHTCHIAN, *Exkmc: Expanding explainable k-means clustering*, arXiv preprint arXiv:2006.02399, (2020).
  - [12] A. GHOSE, *compactem*, Nov. 2020. Software available at <https://compactem.readthedocs.io/en/latest/index.html>.
  - [13] A. GHOSE AND B. RAVINDRAN, *Learning interpretable models using an oracle*, CoRR, abs/1906.06852 (2019).
  - [14] A. GHOSE AND B. RAVINDRAN, *Interpretability with accurate small models*, Frontiers in Artificial Intelligence, 3 (2020).
  - [15] C. GUPTA, A. S. SUGGALA, A. GOYAL, H. V. SIMHADRI, B. PARANJPE, A. KUMAR, S. GOYAL, R. UDUPA, M. VARMA, AND P. JAIN, *ProtoNN: Compressed and accurate kNN for resource-scarce devices*, in Proceedings of the 34th International Conference on Machine Learning, D. Precup and Y. W. Teh, eds., vol. 70 of Proceedings of Machine Learning Research, PMLR, 06–11 Aug 2017, pp. 1331–1340.
  - [16] JAMES BERGSTRA, DAN YAMINS, AND DAVID D. COX, *Hyperopt: A Python Library for Optimizing the Hyperparameters of Machine Learning Algorithms*, in Proceedings of the 12th Python in Science Conference, Stéfan van der Walt, Jarrod Millman, and Katy Huff, eds., 2013, pp. 13 – 19.
  - [17] G. KE, Q. MENG, T. FINLEY, T. WANG, W. CHEN, W. MA, Q. YE, AND T.-Y. LIU, *Lightgbm: A highly efficient gradient boosting decision tree*, in Proceedings of the 31st International Conference on Neural Information Processing Systems, NIPS’17, USA, 2017, Curran Associates Inc., pp. 3149–3157.
  - [18] D. P. KINGMA AND J. BA, *Adam: A method for stochastic optimization*, in 3rd International Conference on Learning Representations, ICLR 2015, San Diego, CA, USA, May 7-9, 2015, Conference Track Proceedings, Y. Bengio and Y. LeCun, eds., 2015.
  - [19] M. KUSNER, S. TYREE, K. WEINBERGER, AND K. AGRAWAL, *Stochastic neighbor compression*, in Proceedings of the 31st International Conference on Machine Learning, E. P. Xing and T. Jebara, eds., vol. 32 of Proceedings of Machine Learning Research, Beijing, China, 22–24 Jun 2014, PMLR, pp. 622–630.
  - [20] E. S. LABER, L. MURTINHO, AND F. OLIVEIRA, *Shallow decision trees for explainable k-means clustering*, CoRR, abs/2112.14718 (2021).
  - [21] M. MOSHKOVITZ, S. DASGUPTA, C. RASHTCHIAN, AND N. FROST, *Explainable k-means and k-medians clustering*, in Proceedings of the 37th International Conference on Machine Learning, H. D. III and A. Singh, eds., vol. 119 of Proceedings of Machine Learning Research, PMLR, 13–18 Jul 2020, pp. 7055–7065.
  - [22] F. PEDREGOSA, *Hyperparameter optimization with approximate gradient*, in Proceedings of the 33rd International Conference on International Conference on Machine Learning - Volume 48, ICML’16, JMLR.org, 2016, p. 737–746.
  - [23] F. PEDREGOSA, G. VAROQUAUX, A. GRAMFORT, V. MICHEL, B. THIRION, O. GRISEL, M. BLONDEL, P. PRETTENHOFER, R. WEISS, V. DUBOURG, J. VANDERPLAS, A. PASSOS, D. COUNAPEAU, M. BRUCHER, M. PERROT, AND E. DUCHESNAY, *Scikit-learn: Machine learning in Python*, Journal of Machine Learning Research, 12 (2011), pp. 2825–2830.
  - [24] J. C. PLATT, *Probabilistic outputs for support vector machines and comparisons to regularized likelihood methods*, in ADVANCES IN LARGE MARGIN CLASSIFIERS, MIT Press, 1999, pp. 61–74.
  - [25] T. SCHEFFER, C. DECOMAIN, AND S. WROBEL, *Active hidden markov models for information extraction*, in Advances in Intelligent Data Analysis, F. Hoffmann, D. J. Hand, N. Adams, D. Fisher, and G. Guimaraes, eds., Berlin, Heidelberg, 2001, Springer Berlin Heidelberg, pp. 309–318.
  - [26] F. WILCOXON, *Individual comparisons by ranking methods*, Biometrics Bulletin, 1 (1945), pp. 80–83.
  - [27] W. ZHANG, X. CHEN, Y. LIU, AND Q. XI, *A distributed storage and computation k-nearest neighbor algorithm based cloud-edge computing for cyber-physical-social systems*, IEEE Access, 8 (2020), pp. 50118–50130.

# Supplementary Text for “Accurate Small Models via Adaptive Sampling”

Abhishek Ghose

## 1 Additional Results

We present plots of comparisons that we were unable to include in the main paper. For each of the experiments - explainable clustering, prototype-based classification, Random Forests - the main paper shows results for one dataset and the mean ranks. Here, comparisons for all datasets, over which the mean ranks were computed, are shown.

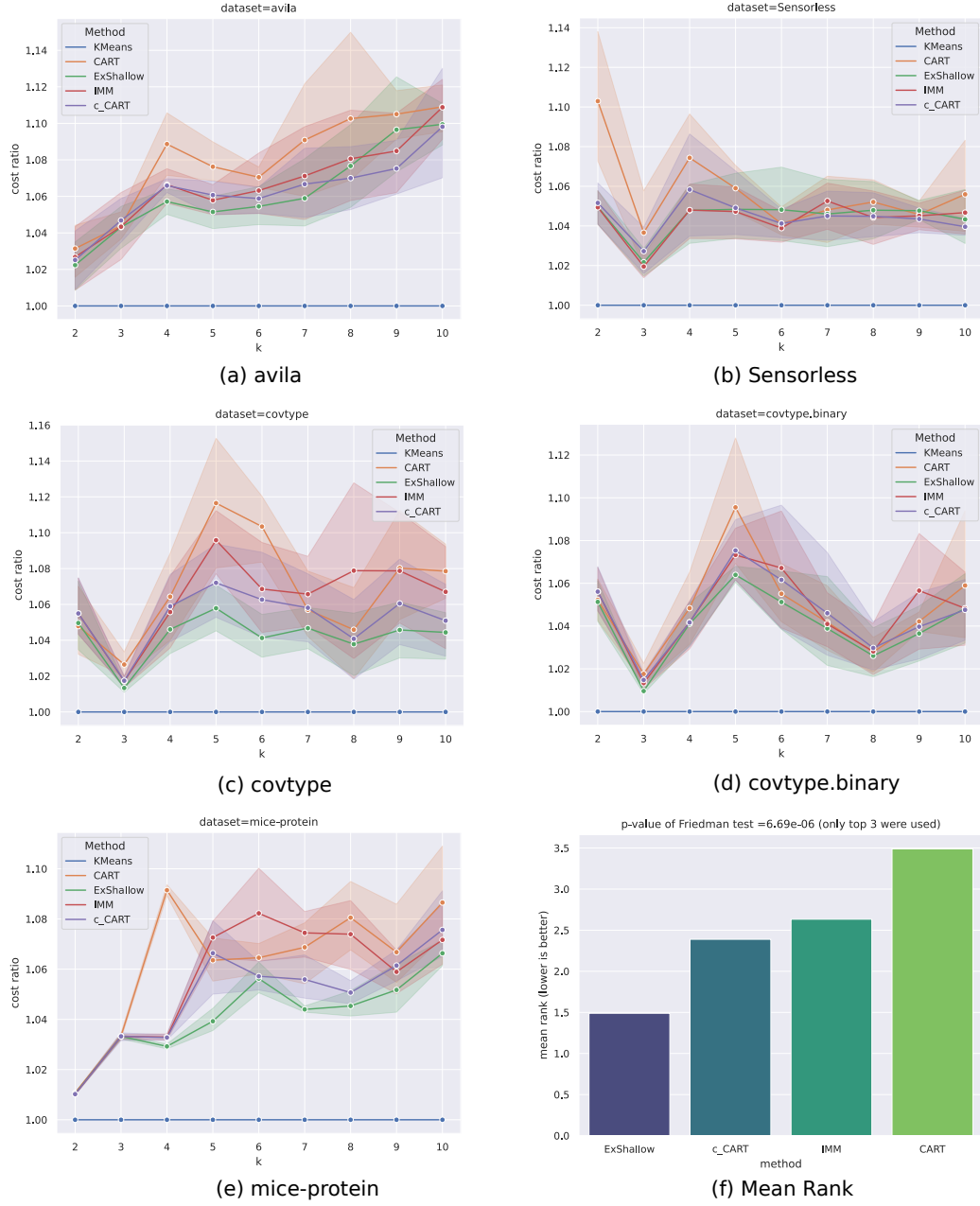


Figure 1: Comparisons over various explainable clustering algorithms are shown. Sub-figures (a), (b), (c), (d), (e) are specific to datasets, mentioned in the title. (f) shows the mean ranks of techniques; the Friedman test is conducted over the **top three** techniques only, with  $p = 6.688 \times 10^{-6}$ .

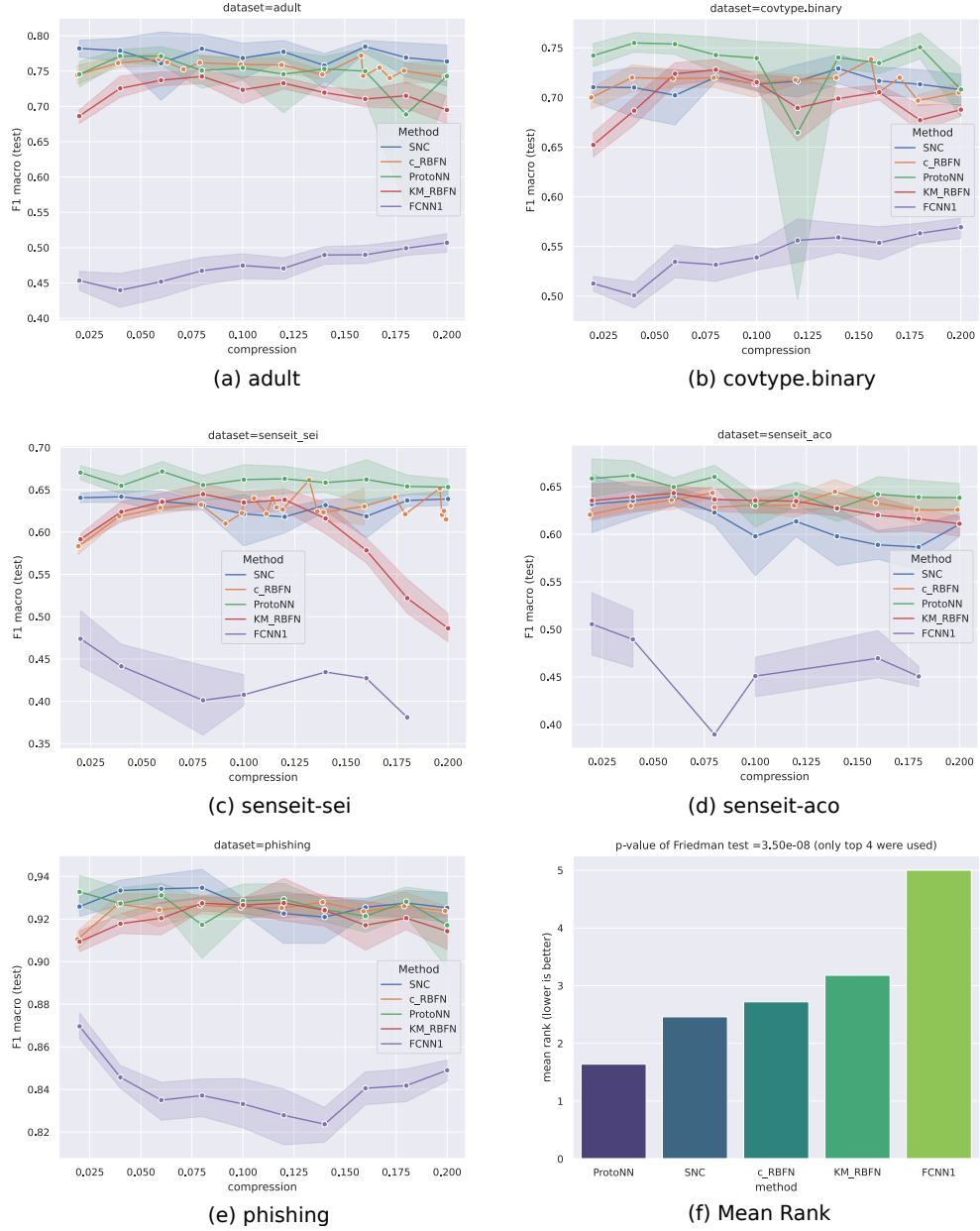
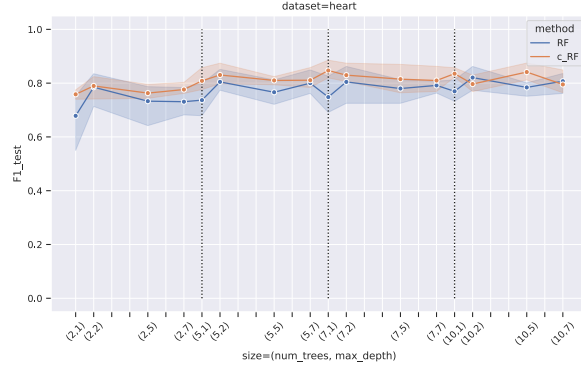


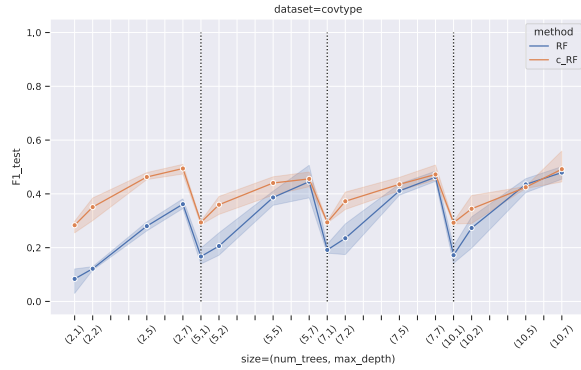
Figure 2: Various prototype-based classifiers are compared. Sub-figures (a), (b), (c), (d), (e) are specific to datasets, mentioned in the title. Number of prototypes are shown as percentage of the training data on the  $x$ -axis. (f) shows the mean ranks of techniques; the Friedman test is conducted over the **top four** techniques only, with  $p = 3.5025 \times 10^{-8}$ .



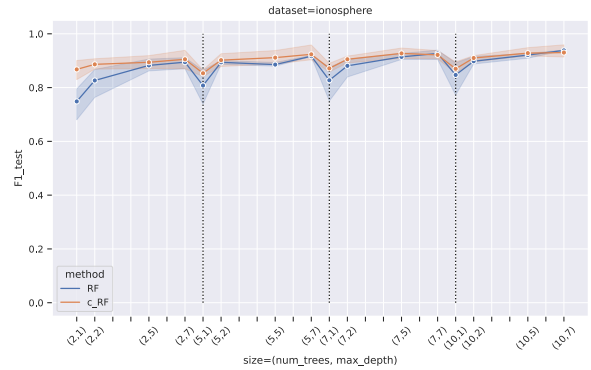
(a) heart



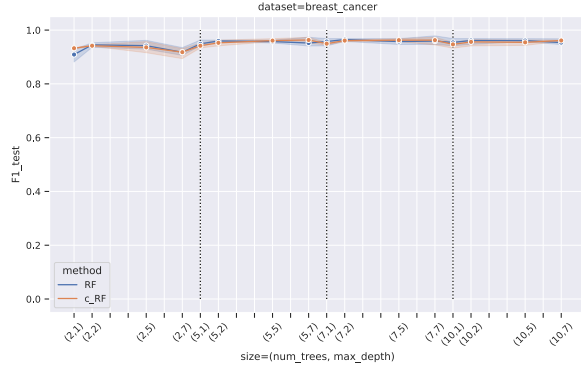
(b) Sensorless



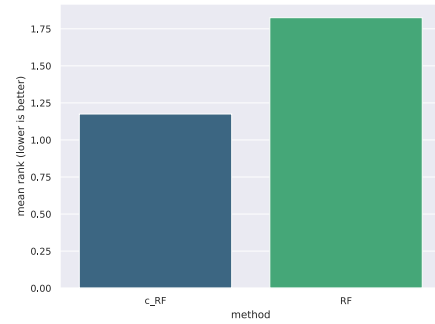
(c) covtype



(d) ionosphere



(e) breast cancer



(f) Mean Rank

Figure 3: (a), (b), (c), (d), and (e) show plots specific to datasets. The  $x$ -axis shows values of the tuple  $(num\_trees, max\_depth)$  sorted by the first and then the second index. The F1-macro score is reported. (f) provides the mean ranks, but since there are only two models being compared, the Friedman test cannot be performed.